International Journal of Engineering & Technology, 7 (4.25) (2018) 119-125

International Journal of Engineering & Technology

Website: www.sciencepubco.com/index.php/IJET

Research paper

Effect of Wing Locations to the Aerodynamic of UiTM's Blended Wing Body-Unmanned Aerial Vehicle (BWB-UAV) Prototype

Farah Diyana Nasri Huang[1], Wirachman Wisnoe[1]*, Rizal Effendy Mohd. Nasir[1], Ehan Sabah Shukri Askari[2]

[1]Flight Technology and Test Centre (FTTC), Faculty of Mechanical Engineering, Universiti Teknologi MARA (UiTM), 40450 Shah Alam, Selangor DE, Malaysia
[2]Engineering Technical College-Baghdad, Middle Technical University (MTU), Baghdad, Iraq
**Corresponding author E-mail: wira_wisnoe@salam.uitm.edu.my*

Abstract

This paper focuses on the effect of wing placement on UiTM's BWB Prototype to the aerodynamic performance of the aircraft. Lift coefficient (C_L), drag coefficient (C_D) and pitching moment coefficient (C_M) are analyzed at 20 m/s air velocity, using NUMECA Computational Fluid Dynamics (CFD) software. Three wing locations are selected, i.e.: initial location (in reference to the BWB Prototype), front location (30% from leading edge), and middle location (in between of the first two cases). The canard and wing tips from the BWB Prototype are removed for this study. Grid independence study is completed to observe the effect of number of cells on the computation results. Comparison between the CFD and wind tunnel results on the initial BWB Prototype is performed for validation purpose. The variation of C_L, C_D and C_M are presented in curves of lift coefficient, drag coefficient and pitching moment coefficient against angles of attack (α). The lift coefficient curves give similar trends for the three wing locations and the initial configuration except between 20° – 35° angles of attack where different fluctuation behavior occurs on the curves. The maximum lift coefficient obtained is around 0.86 – 1.05 at α = 26° – 30°. Drag coefficient curves also show similar trend for the three wing locations, but lower than the initial configuration due to removal of the canard and wing tips. The pitching moment curves show significant difference in slope among the three placements of the wing for α above 10°. The pitching moment coefficient curves indicates negative slopes up to of α = 18° (initial and middle case) and α = 22° (front case) which indicates static stability for all cases. Curves show that the middle wing configuration continues to give static stability up to higher angles of attack whereas the front case provides the best static stability up to α = 22°. Overall the absence of canard and wing tips removes the sudden change of slope of pitching moment around α = 12° which initially occurs on the BWB-UAV Prototype.

Keywords: *Aerodynamic; Blended Wing Body; Computational Fluid Dynamics; Unmanned Aerial Vehicle; wing locations*

1. Introduction

Blended Wing Body (BWB) is an idea where the fuselage of an aircraft blends with the wing and tail, forming a hybrid shape that resembles a flying wing [1]. The idea behind it is that the BWB is able to provide a single lifting surface by stretching the entire wing span of the aircraft [2]. Drag also reduces due to the smooth blended surface of the fuselage and wings which increases its aerodynamic efficiency, as compared to the additional drag that is created on the mating surfaces of the wing and fuselage of a conventional aircraft [3]. With a good shape and configuration, a BWB aircraft can burn 27% lower fuel, have 15% lower take-off weight, 12% lower empty operating weight, 27% lower total thrust, and 20% higher lift-to-drag ratio. These are among the advantages that BWB offers over conventional aircraft [4]. However, the absence of tail section on the BWB contributes to stability issues, especially towards the pitching of the aircraft [3].

Multiple research and development (R&D) had been conducted by Universiti Teknologi MARA (UiTM) on the Blended Wing Body (BWB) Unmanned Aerial Vehicle (UAV) which covers BWB Baseline-I [5], BWB Baseline-II [6], BWB Baseline-III, BWB Baseline-IV and BWB Baseline-V, all of which were fine-tuned differently to study their aerodynamic performance. A BWB-UAV aircraft was then developed and fabricated as an evolution of Baseline-II called the BWB Prototype [7]. The wing span was maintained, while the chord wing was broadened and the body was slimmed down. This makes the BWB Prototype to have a simple planform (Fig. 1).

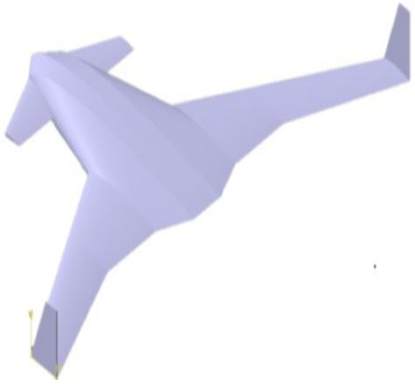

(a) BWB Prototype visualized in CATIA software

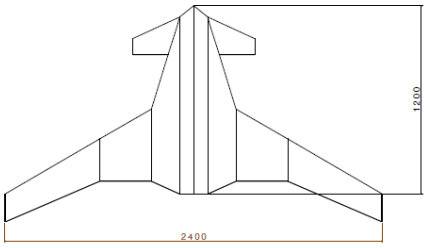

(b) Length and wing span of the BWB Prototype
Fig. 1: BWB Prototype

A series of flight tests had been conducted for the BWB Prototype. The observation made was that the BWB seemed to have longitudinal stability issues. The BWB was able to take off for a few feet from the ground for a few seconds. However, still at zero angle of attack, the nose of the BWB suddenly went down making the BWB to touch the ground again (Fig. 2).

Fig. 2: BWB Prototype with nose down

When the situation described above was overcome (with the help of strong deflection of elevator located at the front (canard)), after a certain angle of attack, an excessive overturning moment was created making the nose of the BWB continue to go up (Fig. 3). The front elevator at the canard cannot be used to rectify the attitude of the aircraft.

Fig. 3: Extreme pitch up moment during takeoff

The fuselage of the BWB uses symmetrical airfoil (NACA0015) that produces zero lift at zero angle of attack (AOA), while the wing uses a cambered airfoil (NACA2412) which produces lift at zero angle of attack. The wing is located at rear part of the aircraft. This means, at zero angle of attack, the wing produces upward lift at the rear part of the aircraft, while the fuselage does not produce any lift. On the other hand, from the side profile of the BWB, the probability to have CG far in front of the aerodynamic center is high due to availability of more space at the front part of the fuselage (Fig. 4). This creates negative pitching moment that makes the aircraft to have nose down.

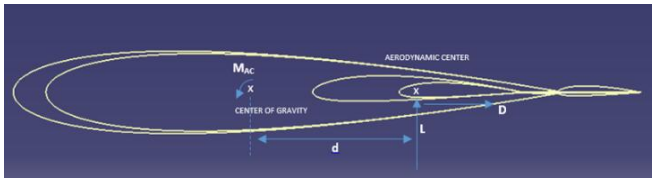

Fig. 4: Position of Lift, Drag and Moment of BWB at zero angle of attack

The negative pitching moment can be reduced by bringing the CG closer to the aerodynamic center. However, moving backward the CG will make the overturning problem explained above worst while it may not be an option due to limited available space at the back of the aircraft. Therefore, moving the aerodynamic center forward would be a solution. This could be done by moving the wing forward.

From further investigation using flow visualization, it was observed that, at $\alpha = 12°$, the outer part of the wing and the canard started to stall [8]. This is a condition where the flow detaches from the surface. At the same time, the flow is still attached on the surface of the fuselage. In this situation, the wing and the canard lost their lifts, while the fuselage produced positive (upward) lift. This condition moves the aerodynamic center of the aircraft forward to the front of the center of gravity (CG) of the aircraft which is located around the location of the wing. This creates a positive moment that makes the nose of the BWB go up.

Moving CG in front of the aerodynamic center of the fuselage will eliminate the overturning moment when the wing is in stall condition. However, without moving the wing forward, it will make the nose of the aircraft too heavy for other AOA making it impossible to fly. In this case, the wing also needs to be moved forward in order to move the aerodynamic center of the whole aircraft closer to the CG. The static and dynamic stability of an aircraft can be achieved by placing the center of gravity (CG) ahead of the aerodynamic center during all flight phases [9].

From the above observation and hypothesis, the two conditions indicating the longitudinal instability are due to the improper force distribution around the aircraft with respect to the center of gravity. Improving the force distribution can eliminate this instability. The location of the wing influences local forces distribution on the aircraft. The force distribution determines the position of the aerodynamic center where the resultants of aerodynamic forces are applied. These resultant forces produce either positive or negative pitching moment with respect to the center of gravity. If an optimum combination of locations of the wing (aerodynamic center) and CG is obtained, the instability issue can be eliminated or at least minimized. This being said, the objective of the paper is to analyze the aerodynamic characteristics and performance of the Blended Wing Body (BWB) for different positions of the wing, particularly towards solving the problems of nose down and nose up of the aircraft as explained above. The stall phenomenon on the wing at certain angles of attack is also highlighted in this paper.

2. Methodology

2.1. Preparation of CAD Drawing

This involves the preparation of three different CAD drawings using the engineering software CATIA, version V5R21. Generally, all three designs have the same length and wingspan of 1.2 m and 2.4 m, respectively. The drawings involve different placements of wings on the fuselage of the BWB. The first drawing (initial case) replicates the aircraft of the BWB Prototype, excluding the wing tips and canards (Fig. 5).

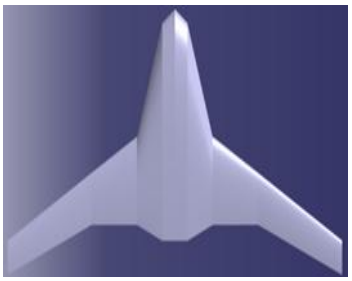

Fig. 5: Initial Case

The next design (front case) involves 30% of each airfoil parts forming the fuselage which were aligned to be in a straight manner. This particular position is chosen as airfoil NACA 0015 and NACA 2412 is thickest at 30% of its total length. Fig. 6 below illustrates the positioning of the aircraft for the front case.

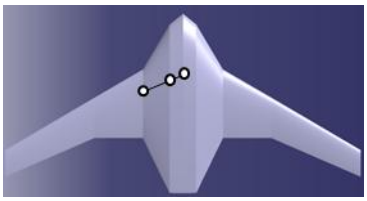

Fig. 6: Front Case

The last position is in between the first two cases, which is middle case as presented in Fig. 7.

Fig. 7: Middle Case

2.2. CFD Setup

In the pre-processing stages, HEXPRESS™ is used to achieve the best possible meshing quality for the aircraft. This is important in order to obtain an accurate result in the computation stages.

2.2.1. Domain

The domain is set up to be the complement of the BWB aircraft body. A simple, rectangular domain is chosen to be used for this simulation with dimensions of 7.2 m x 19.2 m x 7.2 m in the x, y and z axis covering half of the BWB (Fig. 8).

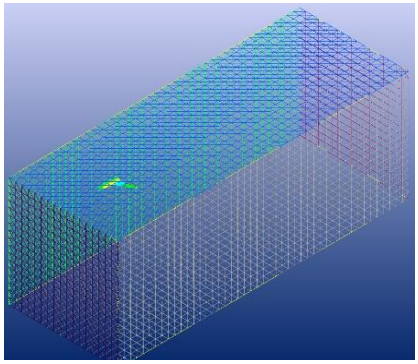

Fig. 8: The domain for the initial case

2.2.2. Meshing

The mesh generation is performed according to a five-step procedure in HEXPRESS™ where each step must be approved before advancing to the next stage. The five stages involved throughout the process are initial mesh, adapt to geometry, snap to geometry, optimize and viscous layers insertion. Below is the completed mesh for the initial, middle and front case (Fig. 9).

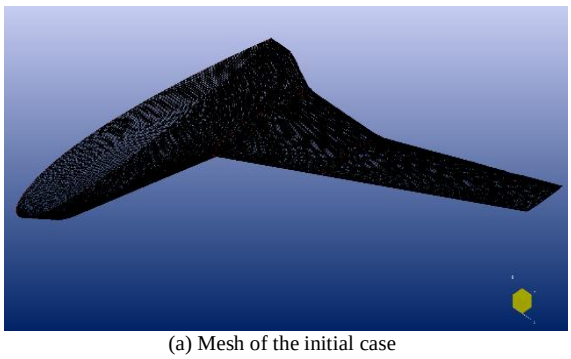

(a) Mesh of the initial case

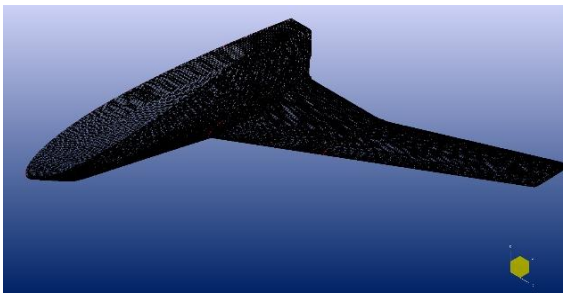

(b) Mesh of the middle case

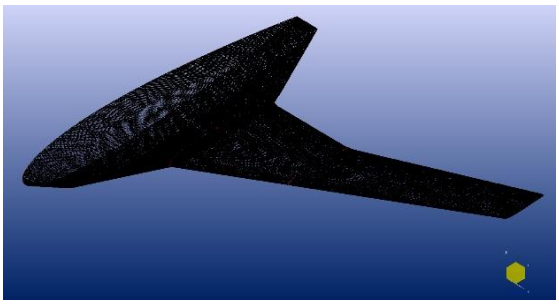

(c) Mesh of the front case

Fig. 9: Complete mesh for the three cases

The generation of accurate results in the computation section depends on the quality and properties of the meshing. Based on Table 1, it can be concluded that the mesh is satisfying according to its properties and qualities listed below.

Table 1: Mesh properties and quality

Criteria	Initial Case	Middle Case	Front Case
Negative cells	0	0	0
Concave cells	0	0	0
Twisted cells	0	0	0
Average skewness	83.119°	82.91°	82.229°
Expansion ratio	9.856	10.775	7.387
Number of cells	2 035 082	2 168 650	3 095 151

2.2.3. Computation

FINEOpen™ is used to run the simulations. All three designs are computed with a reference length and area of 1.2 m and 0.5962 m^2 respectively. The parameters were chosen in accordance with the half-body dimensions of the BWB aircrafts. Table 2 below shows the configurations for the fluid model.

Table 2: Fluid Model

General	
Fluid name	Air (Perfect gas)
Velocity	20 m/s
Reynolds Number	1.5287E+006
Reference Parameters	
Pressure	101325 Pa
Temperature	300 K
Mathematical Model	
Flow Model	Turbulent Navier-Stokes
Turbulence Model	Spalart-Allmaras

For each wing location, the moment reference center has the same relative position from the wing root leading edge (Table 3).

Table 3: Moment reference center location (measured from the nose)

Design	Moment reference center location (m)
Initial Case	0.6
Middle Case	0.497
Front Case	0.314

Meanwhile, for the post-processing stage, physical visualization of the pressure contour and velocity flow is completed using the

CFView™ system. Through this, it helps to physically envision the results obtained.

2.3.1 Measurements

All computations are completed at various angles of attack ranging from -10° to 50°, each with an interval of 4°. The results are expressed in curves of C_L, C_D, and C_M against angles of attack. In addition to that, physical visualization using CFView™ is used to complement the curves plotted for better understanding of the phenomena.

3. Grid Independence Study (GIS)

The Grid Independence Study is performed to observe the effect of number of cells towards the computation results. When the computation results are not affected any more by the parameters of the mesh, it can be said that the independence is achieved. Hence, the parameters can be used as references for other simulations, i.e. the three different designs. All the computations for the grid independence study was done with an angle of attack, $\alpha = 0°$. The completed GIS shows small variation of the lift coefficient (Fig. 10), drag coefficient (Fig. 11) and pitching moment coefficient (Fig. 12) with the increase of number of cells. This indicates low dependency of the results to the number of cells.
When $\alpha = 0°$, the fuselage has zero lift, as the body is symmetrical in size thus the lift comes only from the wings but it is very small in value.

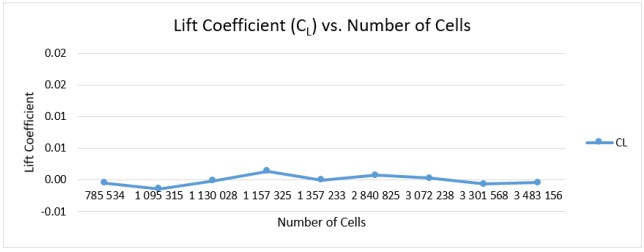

Fig. 10: Lift coefficient vs number of cells

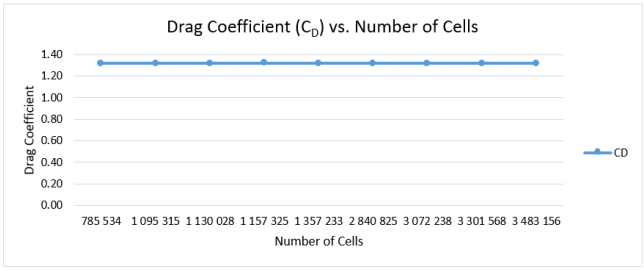

Fig. 11: Drag coefficient vs number of cells

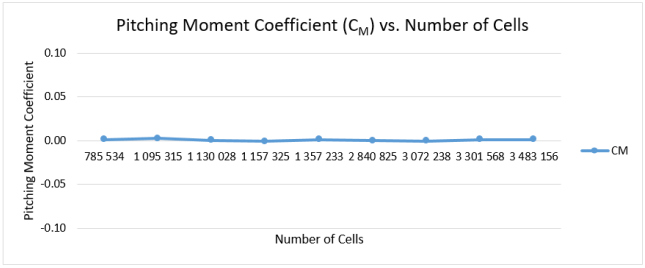

Fig. 12: Pitching Moment coefficient vs number of cells

4. Validation

Validation process is completed by comparing the results obtained from wind tunnel tests with the CFD computation results on the BWB Prototype initial design (with canard and wing tips). The computation is done with the same size of the BWB Prototype wind tunnel model (1/4 of the real size), at an air speed of 20 m/s. The model's reference length is 0.291 m and its reference area is 0.035054 m^2. The results are presented in Fig. 13 and Fig. 14.
From these figures, it is observed that both curves from CFD and wind tunnel have similar trends with only slight deviation at higher angles of attack (above 10° for C_L and above 30° for C_D).

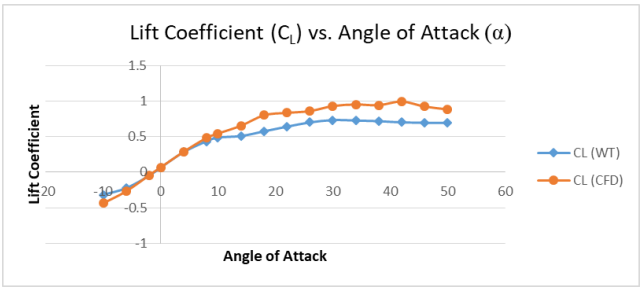

Fig. 13: Lift Coefficient vs angles of attack (α) of BWB Prototype model

In addition to that, the wind tunnel result shows a slight deflection of C_L curve at $\alpha = 12°$ (Fig. 13) which corresponds to the occurrence of stall at the outer wing (visualized using thread tufts visualization) [8]. Meanwhile, the graph representing CFD result does not detect any partial stall at that angle of attack. This might be due to the setting of parameters for the CFD simulation including the selection of turbulence model.

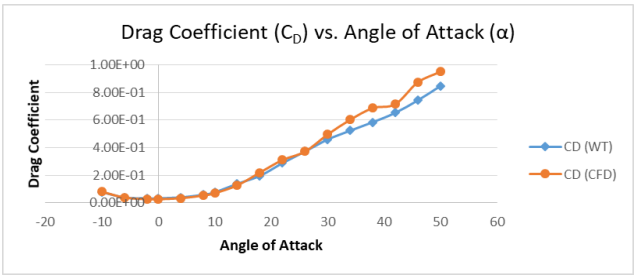

Fig. 14: Drag Coefficient vs angles of attack (α) of BWB Prototype model

5. Results and Discussion

As previously mentioned, computations are carried out for multiple angles of attack (α) between -10° to 50° with an airflow of 20 m/s applied to the three cases of wing location.
The lift and drag coefficient are represented in Fig. 15 and Fig. 16. The CFD results of the BWB-UAV Prototype are also added to the curves [10]. It can be seen that the values of lift coefficient increases with the angle of attack for all cases until it reaches the maximum value at angles 26° and 30°. The lift coefficient reaches maximum at $\alpha = 26°$ for the initial and middle cases with a value of 0.86 and 0.914 respectively. Meanwhile, the front case reaches its maximum value of 1.01 at $\alpha = 30°$. As for the BWB Prototype, it has slightly higher maximum lift coefficient value of 1.05 at $\alpha = 30°$.

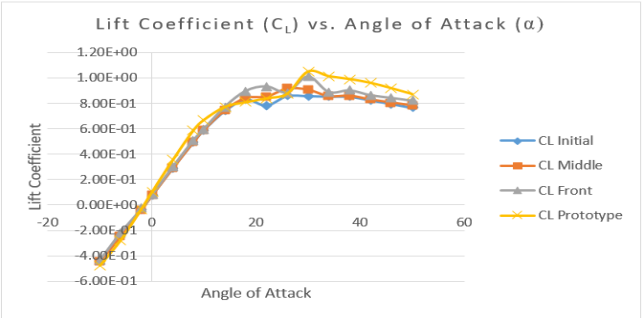

Fig. 15: Graph of Lift coefficient (C_L) vs angles of attack (α)

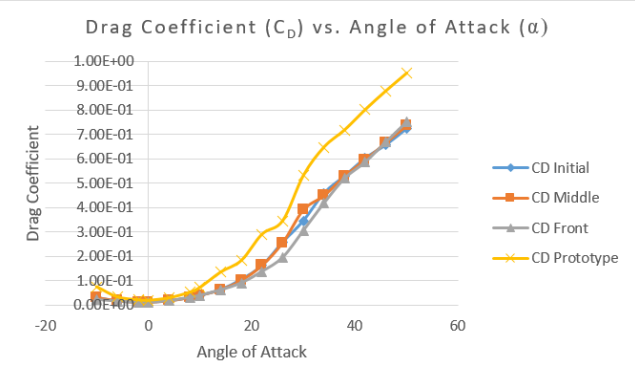

Fig. 16: Graph of Drag coefficient (C_D) vs angles of attack (α)

A sudden deflection in the C_L curve occurs around α = 22° for the initial and middle case whereas at α = 26° for the front case (Fig. 15). According to Fig. 15, the CFD result also does not detect any partial stall in the wing area when α = 12°.

Referring to Fig. 17 and Fig. 18, the velocity profile shows that both cases (initial and middle cases) undergo flow separation at the wing area. This indicates that there is an occurrence of stall on the wing at this particular angle where it loses part of its lift, hence the sudden deflection. Meanwhile, for the front case (α = 26°), it can be seen at two sections of the wing where flow separation also occurs (Fig. 19).

Referring to Fig. 16, the three cases have similar trends of drag coefficient with slight differences from α = 22° to α = 34°. The variation in the value of drag coefficient remains small as long as there is no flow separation. Changes in the steepness of the graph can be observed from α = 22° for the initial and middle case, while for the front case is around α = 26°. It is similar to the graphs of lift coefficient where at the same angle, sudden deflection occurs due to the flow separation. When detachment of flow happens, the drag increases which is represented by the immediate increase in the slopes of the curves.

For both lift and drag coefficient graphs, the trend is similar for all three cases due to the fact that the blended wing body has the same surface area regardless of the wing position. The BWB Prototype has higher drag compared to the three other cases. It becomes more significant at higher angles of attack (> 5°). This is normal, as the Prototype is equipped with canard and wing tips. The canard produces additional drag at higher angles of attack. The lift of BWB Prototype is slightly higher than the three other cases due to the presence of the canard. However, as the canard soon reaches a stall condition, the lift decreases again.

Pressure contour for the initial case (Fig. 17(c)) reflects the maximum lift coefficient that correlates with the graph in Fig. 15. The region below the BWB is visualized in 'red' which indicates high pressure that leads to the maximum lift coefficient. Meanwhile, the contours for the middle and front cases are also presented in Fig. 18(c) and Fig. 19(c).

Referring to the area below the BWB, it can be observed that the front case (Fig. 19(c)) visualizes a wider pressure area as compared to the middle case (Fig. 18(c)). Comparing this with the lift coefficient graph in Fig. 15, it confirms the phenomena where the lift coefficient in the front case (α = 26°) is higher than the middle case (α = 22°) at the particular angle.

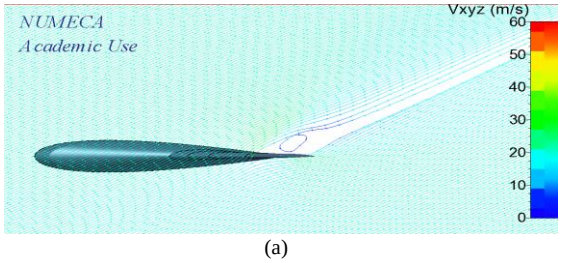

(a)

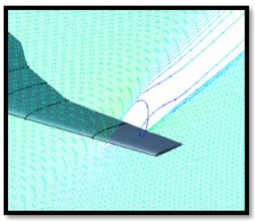

(b)

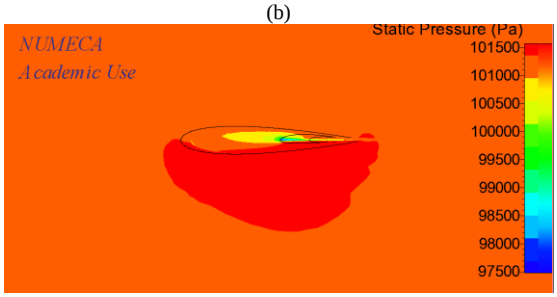

(c)

Fig. 17: (a) Velocity flow, (b) Close-up of velocity flow, (c) Pressure contour at α = 26° (Initial case at maximum lift coefficient)

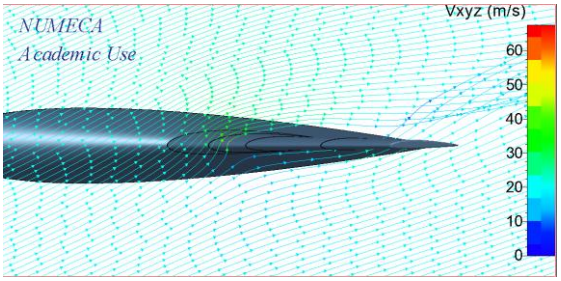

(a)

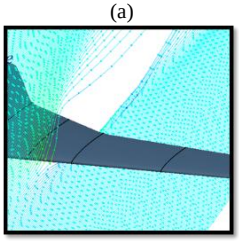

(b)

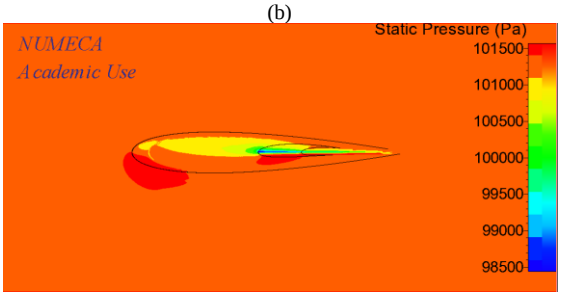

(c)

Fig. 18: (a) Velocity flow, (b) Close-up of velocity flow, (c) Pressure contour at α = 22° (Middle case at deflection)

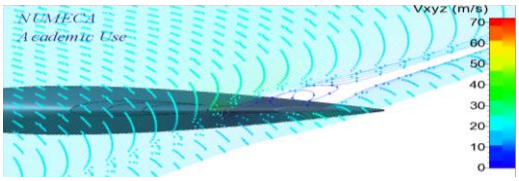

(a)

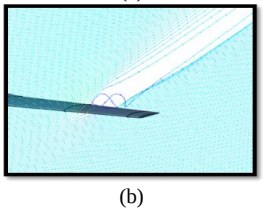

(b)

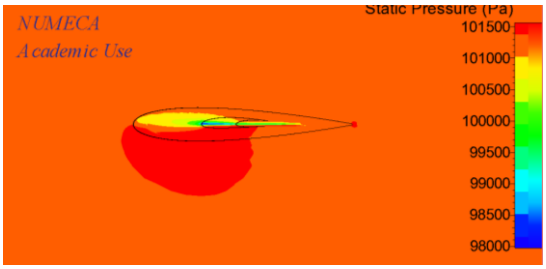

(c)

Fig. 19: (a) Velocity flow, (b) Close-up of velocity flow, (c) Pressure contour at α = 26° (Front case at deflection)

The graph of Pitching Moment Coefficient (C_M) is visualized in Fig. 20 below. All three cases (apart from the BWB Prototype) show almost the same slopes up to α = 10°, and then they start to differ until α around 20° where significant deviation occurs changing the slope from negative to positive.

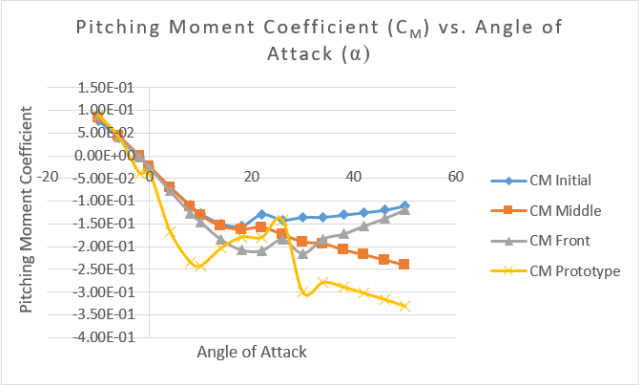

Fig. 20: Pitching Moment Coefficient (C_M) vs angles of attack (α)

At α = 0°, the initial case has a pitching moment coefficient of -0.025, -0.023 for middle case and -0.027 for the front case, which is all around the same range of values. This indicates that although equipped with different wing locations, the aircraft still has a nose down moment at α = 0°. This is because the moment center (the center of gravity) is located in front of the aerodynamics center of the aircraft. The strength of this nose down moment can be reduced by shifting the center of gravity to the back. For initial case, this operation is difficult to be performed as the space available towards the tail of the aircraft is very limited. However, the possibility is quite large for the middle and front cases. Hence, moving the wing forward creates more space to adjust the center of gravity backward.

All three cases show pitching moment deflection of slopes around α = 20°. Improvement in terms of slope deflection compared to the initial BWB Prototype is noticeable. The initial BWB Prototype indicates a strong deflection of slope at around α = 12°. This is due to the stall that occurs at the outer wing which advances the aerodynamic center to the front of the center of gravity, creating a relatively positive moment from the previous situation before the stall occurs. Hence, an overturning moment is created. By removing the canard and by locating the wing forward delays the change of slope to α around 20°. Note that the three wing location cases use the same airfoil as the Prototype, even though it is not observed clearly through CFD simulation, the visualization results from reference [8] suggest that stall should start occurring around α = 12° at the outer wing regardless the location of the wing.

The slopes of the initial and middle cases start to deflect from negative to positive around α = 18°. The front case maintains the negative slope further up to α = 22°. All cases suggest that the aircraft is statically stable up to these angles with its center of gravity in front of the aerodynamic center. The front case gives better static stability, as steeper the negative slope, better the stability is [11]. The initial and front cases produce positive slopes after α = 26° and α = 30° respectively that will affect the static stability of the aircraft. Overturning moments will still occur for the initial and front cases.

A different trend is shown by the middle case. From α = 18° to α = 22°, the curve shows almost zero slope indicating that the pitching moment is independent of the angle of attack. In this case, the center of gravity and the aerodynamic center are at the same location. The curve produces negative slope afterwards, indicating that the aerodynamic center is moving backward again behind the center of gravity. The curve suggests there is no overturning moment for the middle case.

6. Conclusion

Aerodynamic analysis of UiTM's BWB-UAV aircraft with three different wing locations was completed through CFD. The lift, drag and pitching moment coefficients were obtained and presented in curves against various angles of attack together with the initial BWB Prototype. Grid independence study was performed showing almost independent results for the range of number of cells used. Parameter validation indicates the CFD results to be in line with the wind tunnel test results. However, the CFD fails to show the partial stall at the outer wing at α = 12°. Graphs of lift and drag coefficient plotted shows a similar trend among the three wing locations. The removal of the canard does not change much the value of lift, but significantly reduces the drag. From the pitching moment curves, the initial and front case were unable to retain its stability after α = 18° (initial case) and α = 22° (front case) which can be seen through positive slope in the curves. Meanwhile, the middle case maintains a good static stability by keeping negative and zero slope throughout all angles of attack.

Overall, the nose down moment at α = 0° can be reduced by moving the center of gravity backward towards the aerodynamic center which practically can be done for middle and front case. Meanwhile, the overturning moment at higher angles of attack is avoided for the middle case. On the other hand, if the aircraft is considered to fly with angles of attack only up to α = 22°, the front case is considered to be better as the curve shows steepest slope among all three cases, providing better static stability.

Acknowledgement

The authors would like to thank the Faculty of Mechanical Engineering, Universiti Teknologi MARA (UiTM) for providing assistance and support for this research.

References

[1] H. Djojodihardjo and A. K. L. Wei, "Hybrid Wing Body Business Jet Conceptual Design and Aerodynamic Study", International Journal of Mechanical and Mechatronics Engineering, vol. 15, no. 2, pp. 42–55, 2015.

[2] P. Mahamuni, A. Kulkarni, and Y. Parikh, "Aerodynamic Study of Blended Wing Body", International Journal of Applied Engineering Research (IJAER), vol. 9, no. 24, pp. 29247–29255, 2014.

[3] D. J. Thompson, J. Feys, M. D. Filewich, S. Abdel-magid, D. Dalli, and F. Goto, "The Design and Construction of a Blended Wing Body UAV", 49th AIAA Aerospace Sciences Meeting including the New Horizons Forum and Aerospace Exposition, Aerospace Sciences Meetings. January 4-7, 2011, Orlando, Florida, no. January, pp. 841–851, 2011.

[4] E. Ordoukhanian and A. M. Madni, "Blended wing body architecting and design: Current Status and Future Prospects", Procedia Computer Science, vol. 28, pp. 619–625, 2014.

[5] W. Wisnoe, W. Kuntjoro, F. Mohamad, R. E. M. Nasir, N. F. Reduan, and Z. M. Ali, "Experimental Results Analysis for UiTM BWB Baseline-I and Baseline-II UAV Running at 0.1 Mach number", International Journal of Mechanics, vol. 4, no. 2, pp. 23–32, 2010.

[6] W. Wisnoe, R. E. Nasir, R. Ramly, W. Kuntjoro, and F. Muhammad, "Aerodynamic of UiTM's Blended Wing Body Unmanned Aerial Vehicle Baseline-II Equipped with One Central Vertical Rudder", Jurnal Teknologi, vol. 4, pp. 95–99, 2015.
[7] W. Wisnoe, W. Kuntjoro, R. E. Mohd Nasir, F. Mohamad, R. Ramly, and A. M. I. Mamat, "Blended Wing-Body Micro-Class Unmanned Aircraft Prototype for Aerial Surveillance", Prototype Research Grant Scheme (PRGS) Report, 2017.
[8] W. Wisnoe, R.E.M. Nasir, W.A.M. Saarani, N. Mohd Saad, and M.A.A. Mamud, "Wind Tunnel Tests of UiTM Blended Wing Body - Unmanned Aerial Vehicle (BWB-UAV) Prototype", Journal of Mechanical Engineering, SI 4(3), pp. 234-245, 2017.
[9] A. Baig, T. Cheema, Z. Aslam, Y. Khan, H. Sajid Dar, and S. Khaliq, "A New Methodology for Aerodynamic Design and Analysis of a Small Scale Blended Wing Body", Journal of Aeronautics & Aerospace Engineering, vol. 7, no. 1, pp. 1–6, 2018.
[10] M. A. Mohamad Sanusi, "Study on Pitching Behaviour of UiTM's BWB UAV Prototype", Final Year Project Report, Faculty of Mechanical Engineering, Universiti Teknologi MARA, 2015.
[11] F. Hitchens, "The Encyclopedia of Aerodynamics", Andrews UK Limited, 2015.